

Research Article

Location Design of Electrification Road in Transportation Networks for On-Way Charging

Yue Qiu,¹ Yuchuan Du ,¹ Shanchuan Yu,² and Shengchuan Jiang¹

¹Key Laboratory of Road and Traffic Engineering of the Ministry of Education, Tongji University, Shanghai 201804, China

²China Merchants Chongqing Communications Research & Design Institute Co. Ltd., Chongqing 400067, China

Correspondence should be addressed to Yuchuan Du; yctu@tongji.edu.cn

Received 18 January 2020; Revised 14 March 2020; Accepted 26 June 2020; Published 23 July 2020

Academic Editor: Wei (David) Fan

Copyright © 2020 Yue Qiu et al. This is an open access article distributed under the Creative Commons Attribution License, which permits unrestricted use, distribution, and reproduction in any medium, provided the original work is properly cited.

Electric vehicles tend to be a great mobility option for the potential benefits in energy consumption and emission reduction. On-way charging (OWC) has been recognized to be a promising solution to extend driving range for electric vehicles. Location of the electrification road (ER) is a critical issue for future urban traffic management to accommodate the new mobility option. This paper proposes a mathematical program with equilibrium constraint (MPEC) approach to solve this problem, which minimizes the total travel time with a limited construction budget. To describe the drivers' routing choice, a path-constrained network equilibrium model is proposed to minimize their travel time and prevent running out of charge. We develop a modified active set algorithm to solve the MPEC model. Numerical experiments are presented to demonstrate the performance of the model and the solution algorithm and analyze the impact of charging efficiency, battery size, and comfortable range.

1. Introduction

Electrification systems based on renewable energy power sources are introduced in the urban transportation system for positive environmental effect and carbon reduction [1, 2]. Recently, with the increasing concern about sustainable transportation [3], electric vehicles (EVs) are widely adopted in urban travel. Electrification road (ER) is considered as a promising domain for sustainable electrical energy harvesting to support on-way charging (OWC) for EVs, thanks to the advancement of application of photovoltaic, piezoelectric, and pyroelectric materials converting solar energy, physical pressure, and thermal energy into electrical energy, e.g., [4–8]. OWC provides a new mode of charging for EV drivers to extend driving range, who are suffering from range anxiety of running out of power on the way [9, 10] and long charging time ranging from 0.5 to 2 hours for a full charge [11]. OWC has raised the interests of organizations and is being tested all over the world. ER deployed on a network has been tested in South Korea [12]. UK has conducted a series of OWC recharging tested on highways [13]. In Sweden, the Volvo Group and the Swedish

Transport Association planned to build 500-meter ER for wireless power transfer [14]. Such tests and experiments show that OWC would come true in future. Owing to the high investment in the ER, which reaches \$4 million per lane mile [15], it is imperative to find the optimal location.

Most previous studies related to the location design of charging facilities are based on user equilibrium (UE) problems with EVs which investigate how the limited driving range of EVs and location of charging facilities affect the routing choice and subsequently the flow equilibrium distribution on road networks. Among these studies, Jiang et al. [16] first proposed a path-constrained assignment model where lengths of selected routes are within the driving ranges of EVs. The model is further extended to consider mixed gasoline and electric vehicle flows and their combined routing choices under different problem settings [17, 18]. He et al. investigated the optimal prices of electricity and the integrated prices of electricity and roads based on the multiclass spatial distribution of electric vehicles across the transportation network [19, 20]. All these studies assumed the energy consumption of EVs is flow-independent.

The aforementioned studies do not consider the location of charging facilities in networks. Problems related to the optimal location of charging stations or battery swapping stations have received much attention. He et al. [21] first proposed a UE-based framework for locating charging stations to maximize social welfare, considering route choices of electric vehicles, and further developed three models of different flow dependencies and energy consumption [22, 23]. Xu et al. [24] defined a network with battery swapping stations where swapping time is independent with charging capacity, considering the impact of queuing to find the best charging strategy. These existing relevant studies are intended for charging stations or battery swapping stations, where EVs reach the station, stop, and get replenished. Such models cannot address issues for OWC directly.

OWC, unlike charging stations or battery swapping stations, can charge EVs during the ride. OWC technology has been implemented in a network in South Korea [12]. A limited number of research studies have been done on the OWC problem to select the optimal ER locations so far. Riemann et al. [25] proposed a mixed-integer nonlinear program to describe the flow-capturing location model considering driver's routing behavior. Chen et al. [26] investigated the optimal deployment of charging lanes based on the speed control of EV drivers on the charging lanes. Chen et al. [27] proposed the integrated deployment of charging lanes and charging stations along a long traffic corridor, which cannot be applied in the transportation network directly. Liu and Song [28] adopted a robust optimization methodology to provide robust location optimization of wireless charging facilities for the electric bus system to reduce total cost of batteries and charging facilities with different uncertainty levels. Liu et al. [29] developed a mixed-integer linear program for OWC location and battery size optimization and battery size for an electric bus system with overlapping bus lines. Ahmed et al. [30] introduced a method to find the best combination of battery capacity and wireless charger characteristics to solve the tradeoff between maximizing charge sustaining, minimum battery capacity, and minimizing the initial investment. Bi et al. [31] adopted a genetic algorithm to optimize the rollout of OWC infrastructure both spatially and temporally in order to minimize life cycle costs and energy burdens. Zhao et al. [32] proposed a biobjective optimization problem for integrated EV location and on-board battery size design of electric bus systems to minimize deployment cost and reduce energy consumption of electrified systems.

The above research studies can solve the ER location optimization to some extent, but they tend to assume that charging amount is only related to the charging time. Under such assumption, drivers tend to deliberately slow down to extend the charging time, and even EV may revisit the same charging lanes. All the vehicles behind the EV that is moving slowly to get charged are delayed. A road contains more than two lanes, one of which is the ER. Vehicles without charging intention would perform lane-changing, which reduces the road capacity. Relationship between the cost of building the ER and width is seldom considered.

In this paper, charging amount is assumed to be related with the driving distance, while charging and the candidates of the ER have to satisfy the minimum energy supply. The width of the ER is considered to affect ER building cost. The link performance function is set as the BPR function in numerical examples. Therefore, the route choice of drivers will be complicated, and the UE flows of EVs in the transportation network will be different.

This paper investigates the location design problem of the ER based on the analysis of the routing behavior of EV drivers, which is different from the previous studies with the charging station or swapping station. Our model inherits from the paper written by He et al. [21], but charging behaviors and routing behaviors are different tracking back to the specific situation of OWC in contrast to charging at station, which leads to a totally different location design. Assuming that the energy consumption rate and recharging rate are flow-independent, this paper proposes a path-constrained network equilibrium model (PCNE) considering the routing and recharging behavior of EV drivers as well as the constraint of driving range. Then, we develop an iterative solution framework to solve the PCNE problem. Lastly, we investigate a mathematical program with equilibrium constraint (MPEC) model to optimize the ER location to minimize the system total travel time under a given construction budget limit. With the proposed model, discussions about the effect of different recharging rates, comfortable ranges, and battery sizes on the location design and system performance are conducted.

The remainder of the paper is organized as follows. The notation, assumption, formulation of the PCNE problem, and a solution framework are elaborated in Section 2. Section 3 formulates the location design problem as a MPEC program. Section 3.1 proposes a modified active set method to solve the problem. Section 4 presents numerical cases based on the Sioux Falls network, and Section 5 offers the conclusions of this study and implications for future research on the transportation network of the ER.

2. Path-Constrained Network Equilibrium Model for On-Way Charging

The section proposes a PCNE model to describe the routing and charging behaviors of EV drivers under a given location design, which determine the network flow pattern. Decision variables of the model include equilibrium flow and charging amount of the EV.

2.1. Notation and Assumption. Following assumptions are made before the model formulation:

Assumption 1. Drivers do not need to revisit the same ER to guarantee that the EV will not be out of charge.

Assumption 2. If the EV is full of charge, charging process stops while running on the ER.

Assumption 3. Given an ER location design, a physical path from the origin to the destination may not be feasible for EV drivers due to the limit for the EV battery.

Assumption 4. All vehicles in networks are EVs. This assumption can be relaxed as the model can be extended to accommodate both EVs and regular vehicles.

Assumption 5. Recharging rate is not affected by speed of the EV.

When EV drivers travel from their origins to destinations, they are assumed to select routes to minimize their travelling cost. Travelling cost includes electricity cost and travel time cost. Electricity cost is much smaller than travel time cost [23]. Therefore, we simply assumed that EV drivers select routes of the least travelling time. While running on the ER, EV drivers can decide whether to charge and charging amount. Charging amount is not greater than the maximum charging amount that equals charging rate multiplied by the distance of the ER.

Consider a transportation network containing ER running EVs, denoted by $G = (N, A)$, where N and A are sets of nodes and link, respectively. The link $(i, j) \in A$ is directional and emanates from the starting node $i \in N$ to the ending node $j \in N$ with the length D_{ij} and the road grade G_{ij} . Travel demands are between a set of O-D pairs W . q^{od} represents the travel demand between the O-D pairs, $od \in W$, and R^{od} represents the set of paths between the O-D pairs.

2.2. Formulation. Following definitions are introduced here to describe the PCNE problem.

Definition 1. A path is usable if an EV is able to complete the path with the remaining charge state never falling below the comfortable range.

EV drivers are assumed to select routes of the least travel time among all the usable paths. At least one usable path exists for each O-D pair here for model generality. As the energy consumption rate and recharging rate are assumed to be flow-independent, the usability of a path is independent of the drivers' routing choice, which can be predetermined before flow distribution given the location design of the ER. The following path-constrained network equilibrium proposed by He et al. [23] is adopted here.

Definition 2. At the path-constrained network equilibrium, all utilized paths are usable, and travel time of all utilized paths of a given O-D pair is the same, which is not more than that of any unutilized usable paths of the same O-D pair.

The formulation of the path-constrained network equilibrium is as follows:

PCNE:

$$\begin{aligned} & \underset{f}{\text{minimize}} && \sum_{(i,j) \in A} \int_0^{\sum_{od \in W} \sum_{r \in R^{od}} f_r^{od} \chi_{i,j,r}^{od}} t_{ij}(z) dz, & (1) \\ & \text{subject to} && \end{aligned}$$

$$\sum_{r \in R^{od}} f_r^{od} = q^{od}, \quad \forall od \in W, \quad (2)$$

$$f_r^{od} \geq 0, \quad \forall od \in W, r \in \widehat{R}^{od}, \quad (3)$$

where \widehat{R}^{od} represents the set of all usable paths between a given O-D pair, $od \in W$. Energy consumption rate and charging rate depend on the travel time, which are flow-independent. Therefore, the usability of any path is flow-independent, which can be calculated. $f = (\dots, f_r^{od}, \dots)$ is a vector of path flow. f_r^{od} represents the traffic flow on path $r \in R^{od}$ of O-D pair, $od \in W$. Constraint (2) demonstrates the flow balance for each O-D pair. Constraint (3) ensures nonnegativity of flow for each usable path.

Here, $\chi_{i,j,r}^{od}$ is a binary variable to represent whether path r traverses link $(i, j) \in A$, which equals 1 if path r traverses link $(i, j) \in A$, and 0 otherwise. v_{ij} represents the traffic flow on the link $(i, j) \in A$. The travel time of link $t_{ij}(v_{ij})$, $(i, j) \in A$, is a strictly increasing function of the flow on link $(i, j) \in A$. Here, assume that link travel time takes the following form of Bureau of Public Roads (BPR):

$$t_{ij} = t_{ij}^0 \left[1 + 0.15 \left(\frac{v_{ij}}{c_{ij}} \right)^4 \right], \quad \forall (i, j) \in A, \quad (4)$$

where t_{ij}^0 represents the free-flow travel time of link (i, j) and c_{ij} represents the capacity of link (i, j) .

2.3. Solution Procedure. If we can enumerate all usable paths beforehand, the proposed PCNE problem is a regular nonlinear optimization which can be solved easily by commercial nonlinear solvers such as CONOPT. However, enumeration of usable paths is a time-consuming work. Here, we adopt the solution procedure proposed by He et al. [22] to obtain the solution. The procedure starts with a subset of \widehat{R}^{od} , $od \in W$, and solves a restricted version of PCNE defined upon the subset. Then, the feasibility of the solution to the restricted PCNE is tested. If not, a new usable path will be generated and added to the subset. Iteration proceeds until termination.

Some new variables are introduced in the subproblem. Here, l_{\max} and l_0 are the battery size and the initial state of charge. For an EV travelling between the O-D pair, $od \in W$, the state of charge at node i is l_i^{od} . δ_{ij} is a binary parameter representing whether link $(i, j) \in A$ is equipped with the ER to support OWC. The variable equals 1 if the street (i, j) is equipped with the ER, and 0 otherwise. $A_p \subseteq A$ denotes the set of all links equipped with the ER. Let ω_{ij} denote the energy consumption rate on link $(i, j) \in A$ and $\bar{\omega}$ denote the recharging rate of the ER. Therefore, link energy consumption is denoted as $c_{ij} = (\omega_{ij} - \delta_{ij} \bar{\omega}) D_{ij}$. m^{od} is the minimum charge state within the comfortable range for drivers of the O-D pair, $od \in W$. $N_t(n)$ is the set of tails of those links heading to node n , and $N_h(n)$ is the set of heads of those links emanating from node n . K and M are sufficient large constants. x_{ij}^{od} is a binary variable indicating utilization incidence, which equals 1 if link (i, j) is utilized for travel demands between the O-D pair, $od \in W$, and 0 otherwise.

Accordingly, ρ_{ij}^{od} is a variable that equals 0 if link (i, j) is utilized for travel demands between the O-D pair, $od \in W$, and is unrestricted otherwise. ξ_{nd} is a binary variable, which equals 1 when $n = d$, and 0 otherwise; ξ_{on} is a binary variable, which equals 1 when $n = o$, and 0 otherwise; and e_{ij}^{od} represents the recharging amount at link $(i, j) \in A$.

For an O-D pair, $od \in W$, the link flow obtained $(\dots, v_{ij}^{[k]}, \dots)$ at the k th iteration of PCNE is adopted at the shortest usable path solution framework (denoted as SUPF- k). The formulation of SUPF- k is shown as follows:

SUPF- k :

$$(x^{[k]}, e^{[k]}) \in \arg \min_{x, e \in \Omega} \sum_{(i,j) \in A} t_{ij}(v_{ij}^{[k]}) x_{ij}^{od}, \quad (5)$$

where Ω consists of the following conditions:

$$\sum_{i \in N_i(n)} x_{in}^{od} - \sum_{j \in N_j(n)} x_{nj}^{od} - \delta_{nd} + \delta_{on} = 0, \quad \forall n \in N, \quad (6)$$

$$l_j^{od} - l_i^{od} + \omega_{ij} D_{ij} - e_{ij}^{od} = \rho_{ij}^{od}, \quad \forall (i, j) \in A, \quad (7)$$

$$0 \leq e_{ij}^{od} \leq D_{ij} \delta_{ij} \omega, \quad \forall (i, j) \in A, \quad (8)$$

$$0 \leq l_n^{od} \leq l_{\max}, \quad \forall n \in N. \quad (9)$$

$$-K(1 - x_{ij}^{od}) \leq \rho_{ij}^{od} \leq K(1 - x_{ij}^{od}), \quad \forall (i, j) \in A, \quad (10)$$

$$l_i^{od} - (\omega_{ij} D_{ij} - e_{ij}^{od}) \geq -M(1 - x_{ij}^{od}) + m^{od}, \quad \forall (i, j) \in A, \quad (11)$$

$$l_o^{od} = l_0, \quad (12)$$

$$\omega_{ij} = \varphi(G_{ij}), \quad \forall (i, j) \in A, \quad (13)$$

$$x_{ij}^{od} \in \{0, 1\}, \quad \forall (i, j) \in A. \quad (14)$$

In the above, the objective function is to minimize the travel time. Constraint (6) guarantees the balance of traffic flow; constraint (7) specifies the relation between the states of the charge of EV batteries travelling from node i to node j , link $(i, j) \in A$. Constraint (8) ensures the recharging amount of electricity on the ER at link $(i, j) \in A_p$ does not exceed the maximum charging quantity that equals charging rate multiplied by the distance of the link. Constraint (9) sets the upper and lower bounds of the states of the charge of the EV. Constraint (10) suggests that the EV driver can only recharge when travelling on the ER. Constraint (11) sets the lower bounds of the states of charge of the EV during the trip to satisfy comfortable range for drivers. Constraint (12) specifies the initial state of charge. Constraint (13) is a given electricity consumption function with respect to the road grade. Constraint (14) requires x_{ij}^{od} to be binary.

The formulation assumes that EV drivers can control the recharging process on the ER. They can determine the

quantity of recharging on the ER. SUPF- k is a mixed-integer linear program, which can be easily solved by commercial solvers like CPLEX 12.8 for small- or medium-sized problems.

The solution to SUPF- k for each O-D pair, denoted as $(\dots, x_{ij}^{od[k]}, \dots, e_{ij}^{[k]}, \dots)$, is adopted in the set construction of the shortest usable path. The iterative steps of PCNE is shown as follows:

Step 0: set the iteration variable $k = 0$ and traffic flow $(\dots, v_{ij}^{[k]}, \dots) = (\dots, 0, \dots)$ for each O-D pair, $od \in W$. Solve SUPF- k to obtain the optimal solution $(\dots, x_{ij}^{od[k]}, \dots, e_{ij}^{[k]}, \dots)$. Construct $\tilde{R}^{od} = \tilde{R}_S^{od[k]}$.

Step 1: solve the restricted NE upon \tilde{R}^{od} . Denote $(\dots, v_{ij}^{[k+1]}, \dots)$ and (\dots, μ^{od}, \dots) as the optimal solutions and multipliers associated with constraint (2).

Step 2: for each O-D pair, $od \in W$, solve SP- $(k+1)$ and obtain the optimal solution, $(\dots, x_{ij}^{od[k+1]}, \dots, e_{ij}^{[k+1]}, \dots)$.

For $\tilde{od} \in W$, if $\mu^{\tilde{od}} > \sum_{(i,j) \in A} t_{ij}(v_{ij}^{[k+1]}) x_{ij}^{\tilde{od}[k+1]}$, $\tilde{R}^{od} = \tilde{R}^{od} \cup \tilde{R}_S^{\tilde{od}[k+1]}$, and go to Step 1, $k = k + 1$. If $\mu^{od} \leq \sum_{(i,j) \in A} t_{ij}(v_{ij}^{[k+1]}) x_{ij}^{od[k+1]}$ for all O-D pairs, terminate and $(\dots, v_{ij}^{[k+1]}, \dots)$ is the equilibrium link flow distribution.

The above procedure terminates in a finite number of steps.

3. Location Design of the ER

This section investigates the location design under a given budget limit to maximize social welfare (i.e., minimize the total travel time of all EVs in our paper). The following assumptions are introduced here.

Assumption 5. Construction cost of the ER is related to length, width of the street.

Assumption 6. When a street is designed to be equipped with the ER, vehicles driving on any lane of the street can get charged. That is, streets in the network are not mixed with charging lanes and regular lanes.

When the ER location is determined, the equilibrium traffic flow can be derived, as well as the recharging and routing behavior. The problem of the location design for electrification road (LDER) is formulated as follows:

LDER:

$$\text{minimize}_{\delta} \sum_{(i,j) \in A} t_{ij}(v_{ij}^*) v_{ij}^*, \quad (15)$$

subject to

$$D_{ij} \delta_{ij} \omega \geq -G(1 - \delta_{ij}) + l_{\max}, \quad (i, j) \in A, \quad (16)$$

$$\sum_{(i,j) \in A} W_{ij} D_{ij} \delta_{ij} B \leq \Theta, \quad (17)$$

$$\delta_{ij} \in \{0, 1\}, \quad (i, j) \in A, \quad (18)$$

$$(f^*, v^*) \in \arg \min_{f \in \Psi(\delta)} \sum_{(i,j) \in A} \int_0^{\sum_{od \in W} \sum_{r \in \widehat{R}^{od}(\delta)} f_r^{od} \lambda_{ij,r}^{od}} t_{ij}(z) dz, \quad (19)$$

where $\Psi(\delta) = \{f \mid \sum_{r \in \widehat{R}^{od}} f_r^{od} = q^{od}, \forall od \in W; f_r^{od} \geq 0, \forall od \in W, r \in \widehat{R}^{od}(\delta)\}$; W_{ij} is the width of link $(i, j) \in A$; B is the construction cost of the unit-area ER, which is the function of the recharging rate ω ; Θ is the budget limit; and G is a sufficiently large constant.

In the above, the objective function represents the total driving time. Constraint (16) presents the shortest length of the street chosen as the ER, guaranteeing that Assumption 1 always holds. Constraint (17) specifies the budget limit for the ER deployment. Constraint (18) requires δ_{ij} to be binary. Constraint (19) states the traffic flow following the result predicted by the PCNE model.

3.1. Active Set Method. LDER is a typical bilevel discrete network design problem with NE at lower level. Many existing solutions from the literature can be explored, for example, branch and bound [33], simulated annealing [34], and SO relaxation [35] with consensus of reformulating an equivalent single-level model with equivalent optimality conditions of the lower-level problem like KKT conditions to find the solution of the bilevel program. Problems with the nonconvex feasible region generally contain many local optimal solutions and typically require a time-consuming branch-and-bound scheme to search for a globally optimal solution. Such algorithms are not readily applicable considering the nonlinear and complementary constraints, adding enormous amount of calculation.

To solve the LDEP, we utilize the active set method [36], which terminates after a finite number of iterations ending with a strongly stationary solution. The active set method has been proved to have the potential for solving larger network design problems. The active set method assigns nonnegative variables in each pair as zero to construct the location design problem as a regular nonlinear program. Adopting multipliers associated with the constraints forcing nonnegative variables to be zero, the proposed algorithm formulates the binary knapsack problem to solve the zero-value assignments to decrease the total travel time.

The active set algorithm starts by setting an initial feasible solution $U = \{\delta_{ij}^0 \mid (i, j) \in A\}$ and considering two sets:

$$\Omega_0 = \{(i, j), \delta_{ij} = 0\}, \quad (20)$$

$$\Omega_1 = \{(i, j), \delta_{ij} = 1\}, \quad (21)$$

where $\Omega_0 \cup \Omega_1 = A$ and $\Omega_0 \cap \Omega_1 = \emptyset$. Under the location design for the ER corresponding to the initial feasible solution U^0 , the NE problem can be solved easily by the path-based iteration procedure proposed in Section 2. Let $V^* = \{v_{ij}^* \mid (i, j) \in A\}$ be the solution set of NE, which is unique because of the monotonically increasing BPR function.

The basic principle of the active set algorithm is to exchange elements between Ω_0 and Ω_1 in order to reduce the overall travel time in each iteration until the system optimal solution is found. In each iteration, the active sets are adjusted to meet the following theorems proved by Zhang et al. [36].

Theorem 1. *Given that Ω_0 and Ω_1 are feasible solution sets, if $\lambda_{ij} < 0$ for some $(i, j) \in \Omega_0$, switching (i, j) from Ω_0 to Ω_1 yields less system travel time. If $\mu_{ij} > 0$ for some $(i, j) \in \Omega_1$, switching (i, j) from Ω_1 to Ω_0 yields less system travel time.*

Theorem 2. *The active set method converges after a finite number of iterations.*

λ_{ij} and μ_{ij} are the Lagrangian multipliers associated with equations (20) and (21), respectively.

To ensure that budget limit and shortest-length limit are satisfied in each iteration according to constraints (16) and (17), an embedded program is proposed as follows:

$$\text{minimize} \quad \sum_{(i,j) \in \Omega_0} \lambda_{ij} g_{ij} - \sum_{(i,j) \in \Omega_1} \mu_{ij} h_{ij}, \quad (22)$$

subject to

$$\begin{aligned} & \sum_{(i,j) \in \Omega_0} D_{ij} g_{ij} \omega + \sum_{(i,j) \in \Omega_1} D_{ij} (1 - h_{ij}) \omega \geq \sum_{(i,j) \in \Omega_0} (-G(1 - g_{ij})) \\ & + \sum_{(i,j) \in \Omega_0} (-G h_{ij} + l_{\max}), \quad \forall (i, j) \in A, \end{aligned} \quad (23)$$

$$\sum_{(i,j) \in \Omega_0} W_{ij} D_{ij} g_{ij} B + \sum_{(i,j) \in \Omega_1} W_{ij} D_{ij} (1 - h_{ij}) B, \quad \forall (i, j) \in A, \quad (24)$$

$$\sum_{(i,j) \in \Omega_0} \lambda_{ij} g_{ij} - \sum_{(i,j) \in \Omega_1} \mu_{ij} h_{ij} \geq \theta, \quad (i, j) \in A, \quad (25)$$

$$g_{ij}, h_{ij} \in \{0, 1\}, \quad \forall (i, j) \in A, \quad (26)$$

where $g_{ij} = 1$ records a shift in $(i, j) \in \Omega_0$ to Ω_1 and $h_{ij} = 1$ records a shift in $(i, j) \in \Omega_1$ to Ω_0 . The objective of programming (22) is to minimize the estimated decrease, the negative value of which implies a potential reduction of the objective value. The process terminates when equation (22) is zero.

Constraint (23) is consistent with constraint (16). Constraint (24) is consistent with constraint (17). Parameter θ is set to guarantee a decrease in the objective function. In the first iteration, $\theta = -\infty$. In the next iteration, θ can be calculated by the following equation:

$$\theta = \varepsilon + \sum_{(i,j) \in \Omega_0} \lambda_{ij} g_{ij} - \sum_{(i,j) \in \Omega_1} \mu_{ij} h_{ij}, \quad (27)$$

where ε is a sufficiently small constant. Equation (27) prevents the solution from degenerating back to the previous iteration by increasing θ by ε .

Set the iteration variable $\eta = 1$, $SO^0 = +\infty$, $TD^0 = -\infty$, and the initial feasible fixed solutions $(\Omega_0^\eta, \Omega_1^\eta)$

Solve (1)–(14) with $(\Omega_0^\eta, \Omega_1^\eta)$ and derive λ_{ij}^η and μ_{ij}^η . Calculate system total travel time SO^η . If $SO^\eta \geq SO^{\eta-1}$, then $\eta = \eta - 1$; go to step 3.

Solve (22)–(26) and $\theta = \varepsilon + TD^{\eta-1}$

If the optimal objective value is zero, $(\Omega_0^\eta, \Omega_1^\eta)$ is the best solution and the iteration ends;

If not, derive (g_{ij}, h_{ij}) and the objective value TD^η and go to step 4.

Obtain a new solution to $(\Omega_0^{\eta+1}, \Omega_1^{\eta+1})$:

$$\Omega_0^{\eta+1} = \Omega_0^\eta - \{(i, j) \in \Omega_0^\eta: g_{ij} = 1\} + \{(i, j) \in \Omega_1^\eta: h_{ij} = 1\}$$

$$\Omega_1^{\eta+1} = \Omega_1^\eta - \{(i, j) \in \Omega_1^\eta: h_{ij} = 1\} + \{(i, j) \in \Omega_0^\eta: g_{ij} = 1\}$$

$\eta = \eta + 1$; go to step 2.

ALGORITHM 1

Steps of the algorithm are shown in the following. Here, SO denotes the objective value of programming (15), and TD denotes the objective value of programming (22). (Algorithm 1).

4. Numerical Examples

4.1. Basic Settings. In this section, numerical examples on the Sioux Falls network in South Dakota are presented to demonstrate the performance of the proposed model as shown in Figure 1, which consists of 24 nodes, 76 links, and 14 OD pairs. All links are available to be equipped with the ER. Table 1 reports the link characteristics, including free-flow travel time (FFTT), width, length, and capacity. The OD demand is given in Table 2.

We assume that the battery size l_{\max} is 25 kWh. The initial state of the charge l_0 is set as 25% l_{\max} . For simplicity, it is assumed that energy consumption rate ω at all links in the network is set as 0.3 (kWh/mile), and the recharging rate $\bar{\omega}$ is set as 2.5 (kWh/mile). The comfortable range for all drivers m^{od} is set as zero. Assume that the cost of building unit-area ER is $(\$2 \times 10^5)/(\text{mile} \times \text{meter})$ at the recharging rate $\bar{\omega} = 2.5$ (kWh/mile). The budget limit Θ is set as \$200,000,000. All the above values are chosen for illustrative purpose. We adopt CPLEX12.8 to solve the PCNE, SP, and LDER.

4.2. Base Case Result. The LDER problem is solved under the aforementioned basic setting, as shown in Figure 2(a). Figure 2(b) depicts the convergence performance of the SP- k algorithm, indicating the potential of the SP- k algorithm in solving the PCNE problem. The equilibrium link flows are reported in Table 3, with the total travel time of 9.20×10^4 h · veh and the average travel time 0.575 h per vehicle.

4.3. Strategy Comparison under Different Budget Limits. In this section, we consider different location designs of the proposed model under different budget limits to demonstrate the system performance, as shown in Figure 3(a). Figure 3 compares the total travel time, cost of the ER, and the number of ERs under different budget limits. As expected, total travel time of the network decreases with an increase in the budget. More ERs are built with an increasing budget when the budget

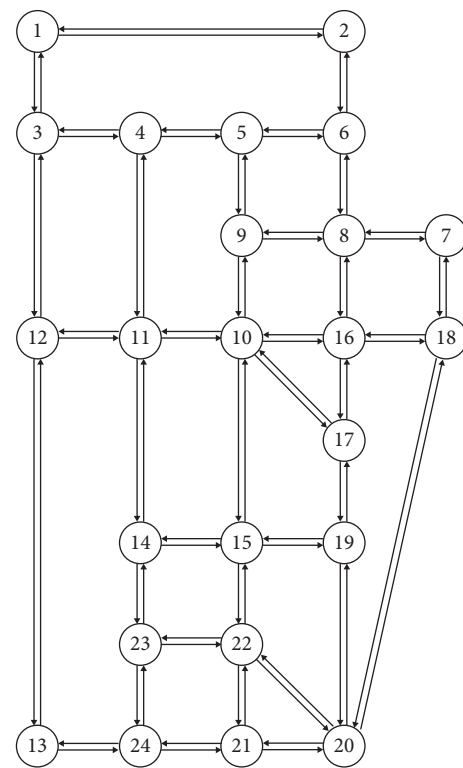


FIGURE 1: Sioux Falls network.

ranges from $\$1.3 \times 10^8$ to $\$2 \times 10^8$, generating more usable route choice for the EV to complete the tour, which promotes average distribution of traffic flow leading to reduction in the system travel time. Nevertheless, more ERs are built under the budget of $\$1.2 \times 10^8$, comparing with the budget of $\$1.3 \times 10^8$ and $\$1.4 \times 10^8$. It can be observed from Figure 3(a) that when the budget exceeds $\$1.4 \times 10^8$, link (20,18) is always chosen to be equipped with ER. The usability of link (20,18) has a significant impact on EV drivers' routing behavior due to its special location. However, ER on link (20,18) of the 15 m width is an expensive project, which has to be weighed according to the budget limit. Figure 3(d) compares the equilibrium link flow of different location designs under different budgets. It can be observed that, under a relatively low budget, the routing choice is limited, which leads to

TABLE 1: Link characteristics: FTTT (min), width (meter), length (mile), and capacity (103 veh/h).

Link	FTTT	Width	Length	Capacity
1-2	6	15	15	25.90
1-3	4	15	10	23.40
2-1	6	15	15	25.90
2-6	5	3.5	12.5	4.96
3-1	4	15	10	23.40
3-4	4	11.25	10	17.11
3-12	4	15	10	23.40
4-3	4	11.25	10	17.11
4-5	2	11.25	5	17.78
4-11	6	3.5	15	4.91
5-4	2	11.25	5	17.78
5-6	4	3.5	10	4.95
5-9	5	7.5	12.5	10.00
6-2	5	3.5	12.5	4.96
6-5	4	3.5	10	4.95
6-8	2	3.5	5	4.90
7-8	3	7.5	7.5	7.84
7-18	2	15	5	23.40
8-6	2	3.5	5	4.90
8-7	3	7.5	7.5	7.84
8-9	10	3.5	25	5.05
8-16	5	3.5	12.5	5.05
9-5	5	7.5	12.5	10.00
9-8	10	3.5	25	5.05
9-10	3	7.5	7.5	13.92
10-9	3	7.5	7.5	13.92
10-11	5	7.5	12.5	10.00
10-15	6	11.25	15	13.51
10-16	4	3.5	10	4.85
10-17	8	3.5	20	4.99
11-4	6	3.5	15	4.91
11-10	5	7.5	12.5	10.00
11-12	6	3.5	15	4.91
11-14	4	3.5	10	4.88
12-3	4	15	10	23.40
12-11	6	3.5	15	4.91
12-13	3	15	7.5	25.90
13-12	3	15	7.5	25.90
13-24	4	3.4	10	5.09
14-11	4	3.5	10	4.88
14-15	5	3.5	12.5	5.13
14-23	4	3.5	10	4.92
15-10	6	11.25	15	13.51
15-14	5	3.5	12.5	5.13
15-19	3	11.25	7.5	14.56
15-22	3	7.5	7.5	9.60
16-8	5	3.5	12.5	5.05
16-10	4	3.5	10	4.85
16-17	2	3.5	5	5.23
16-18	3	15	7.5	19.68
17-10	8	3.5	20	4.99
17-16	2	3.5	5	5.23
17-19	2	3.5	5	4.82
18-7	2	15	5	23.40
18-16	3	15	7.5	19.68
18-20	4	15	10	23.40
19-15	3	11.25	7.5	14.56
19-17	2	3.5	5	4.82
19-20	4	3.5	10	5.00

TABLE 1: Continued.

Link	FTTT	Width	Length	Capacity
20-18	4	15	10	23.40
20-19	4	3.5	10	5.00
20-21	6	3.5	15	5.06
20-22	5	3.5	12.5	5.08
21-20	6	3.5	15	5.06
21-22	2	3.5	5	5.23
21-24	3	3.5	7.5	4.89
22-15	3	7.5	7.5	9.60
22-20	5	3.5	12.5	5.08
22-21	2	3.5	5	5.23
22-23	4	3.5	10	5.00
23-14	4	3.5	10	4.92
23-22	4	3.5	10	5.00
23-24	2	3.5	5	5.08
24-13	4	3.5	10	5.09
24-21	3	3.5	7.5	4.89
24-23	2	3.5	5	5.08

TABLE 2: Network O-D demand (103 veh/h).

O	D	Demand
1	20	16
20	1	16
1	13	8
13	1	8
1	7	12
7	1	12
2	13	10
13	2	10
2	20	8
20	2	8
7	13	14
13	7	14
7	20	12
20	7	12

extremely high traffic flow on some links accompanying considerable travel time, like link 7 and link 35. As budget is increasing, EV drivers have more usable path to select. Equilibrium flow on such links decreases.

4.4. Strategy Comparison with Different Recharging Rates.

In order to investigate the impact of the charging rate on location design and equilibrium flow (see Figure 4), we solve the DLEP and NE with charging rate ω set as 2kWh/mile (LEVEL1), 2.5kWh/mile (LEVEL2), and 3.5kWh/mile (LEVEL3). Cost of the ER is set as $\$1 \times 10^5$, $\$2 \times 10^5$, and $\$3 \times 10^5$, respectively. Budget limit is set as $\$1.9 \times 10^8$. Interestingly, the minimum total travel time can be obtained under this budget in LEVEL 1 and LEVEL 2 cases. That is, even when the budget limit increases, the total travel time will not be reduced. To explore the minimum travel time in LEVEL 3, we repeat to solve the DLEP and NE in the LEVEL 3 case with the budget limit increasing gradually and find the minimum travel time of $9.13 \times 10^4 \text{h} \cdot \text{veh}$ at the budget of $\$2.73 \times 10^8$, which is less than the travel time of $9.20 \times 10^4 \text{h} \cdot \text{veh}$ in the LEVEL 2 case. Figure 4(b) compares the total

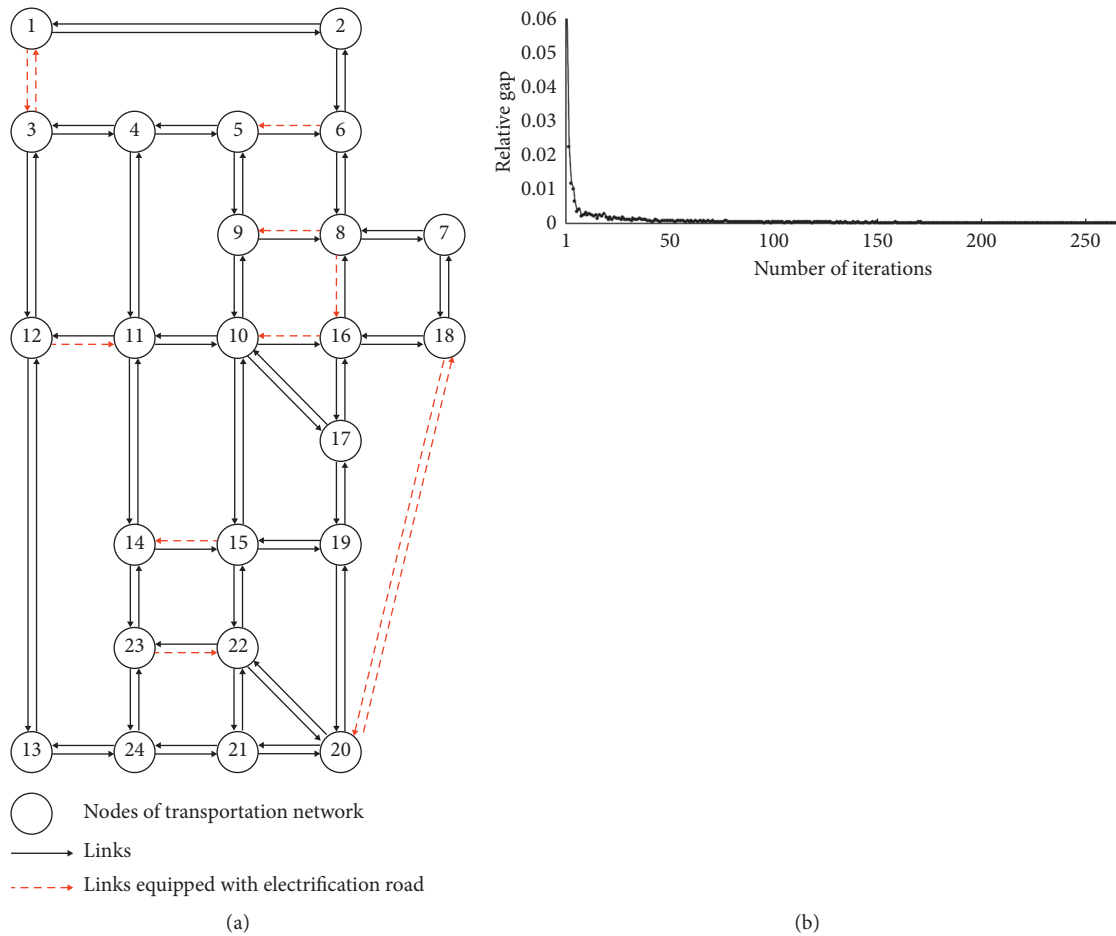


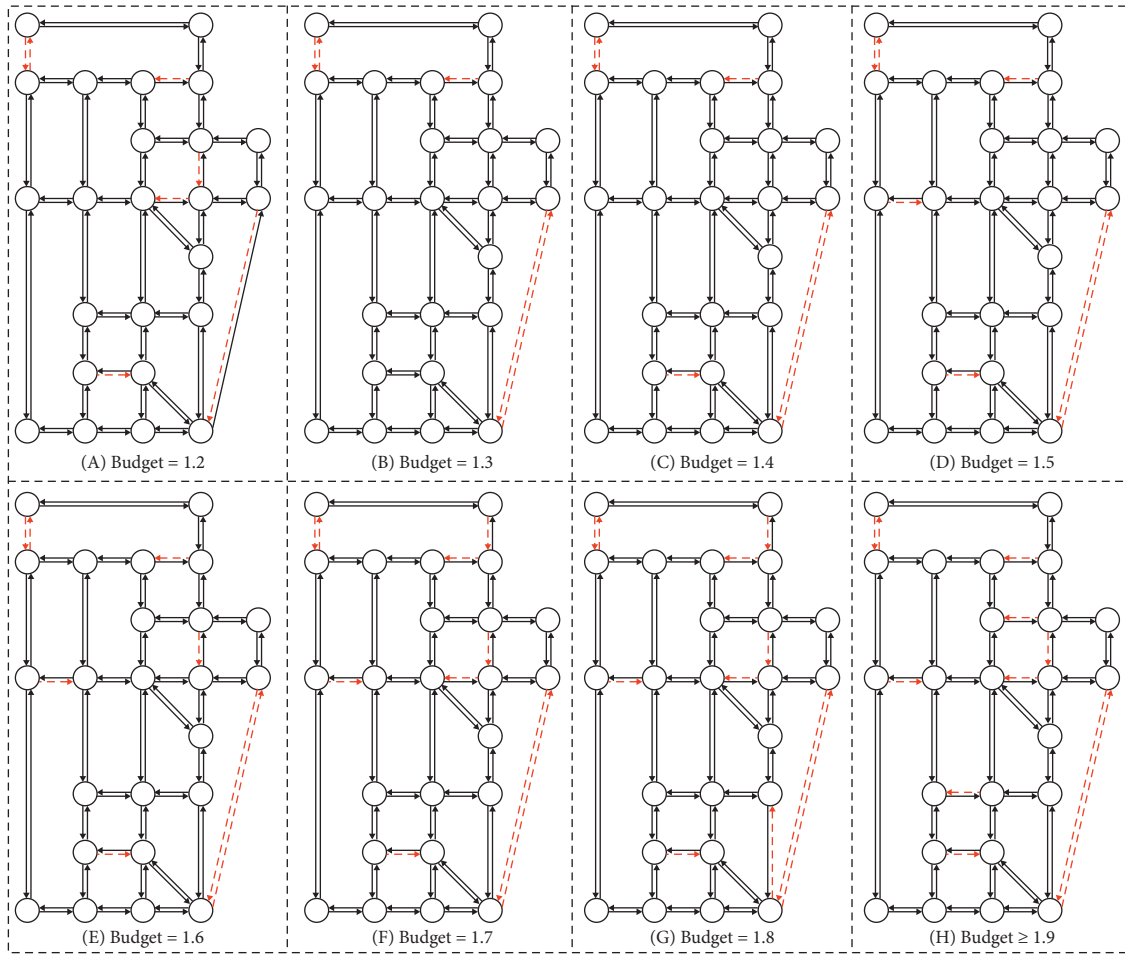
FIGURE 2: Base case result in the Sioux Falls network. (a) Location design of the ER. (b) Performance of the SP algorithm.

TABLE 3: Equilibrium link flow (10^3 veh/h).

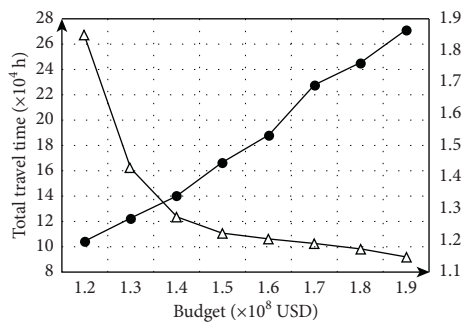
Link	Flow	Link	Flow	Link	Flow	Link	Flow
1-2	10.15	8-7	12.05	13-12	26.68	19-15	6.58
1-3	46.04	8-9	5.99	13-24	10.72	19-17	2.56
2-1	11.36	8-16	6.75	14-11	7.59	19-20	7.78
2-6	7.96	9-5	13.75	14-15	5.34	20-18	31.25
3-1	44.82	9-8	6.10	14-23	0.13	20-19	6.62
3-4	22.77	9-10	6.53	15-10	0.00	20-21	6.09
3-12	23.33	Link	Flow	15-14	7.59	20-22	5.36
4-3	23.45	10-9	7.76	15-19	10.30	21-20	5.33
4-5	17.25	10-11	5.39	15-22	3.91	21-22	0.00
4-11	5.52	10-15	6.35	16-8	5.67	21-24	6.46
5-4	17.47	10-16	8.58	16-10	8.93	22-15	3.52
5-6	5.85	10-17	0.25	16-17	4.22	22-20	6.91
5-9	12.62	11-4	5.98	16-18	17.93	22-21	0.38
6-2	9.18	11-10	8.66	17-10	4.22	22-23	3.98
6-5	4.94	11-12	6.99	17-16	2.81	23-14	0.00
6-8	12.53	11-14	5.47	17-19	0.00	23-22	5.52
7-8	13.33	12-3	21.44	18-7	29.68	23-24	3.98
7-18	28.40	12-11	8.61	18-16	18.60	24-13	10.44
8-6	12.84	12-13	26.96	18-20	29.30	24-21	5.33
						24-23	5.39

travel time and cost in these four cases. It can be observed that, under the budget limit of $\$1.9 \times 10^8$, the ER of LEVEL 2 gets the best performance, which is much better than the

other two cases. Three explanations are offered here. First, due to constraint (16), shortest length of the ER is different as recharging rate changes. In the case of LEVEL 1, only 26

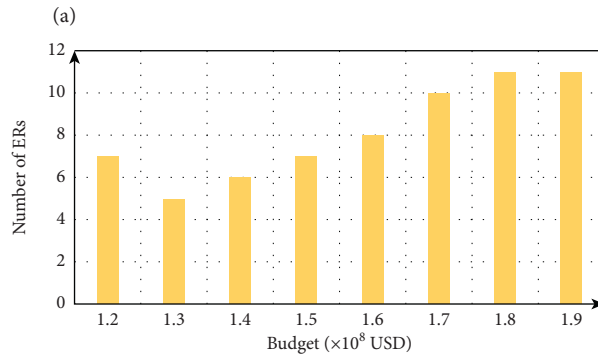


○ Nodes of transportation network
 → Links
 - - - Links equipped with electrification road
 Budget ($\times 10^8$ USD)



△ Total travel time
 ● Cost of ER

(b)



(c)

FIGURE 3: Continued.

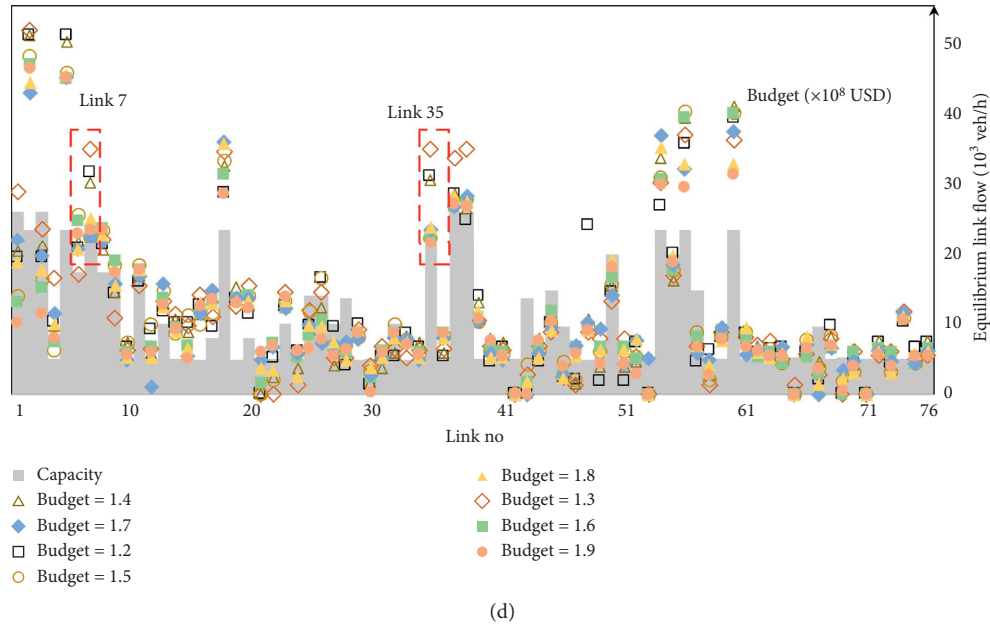


FIGURE 3: Comparison under different budget limits. (a) Comparison of location designs under different budgets. (b) Total travel time and ER cost. (c) The number of ERs under different budgets. (d) Equilibrium flow of different location designs under different budgets.

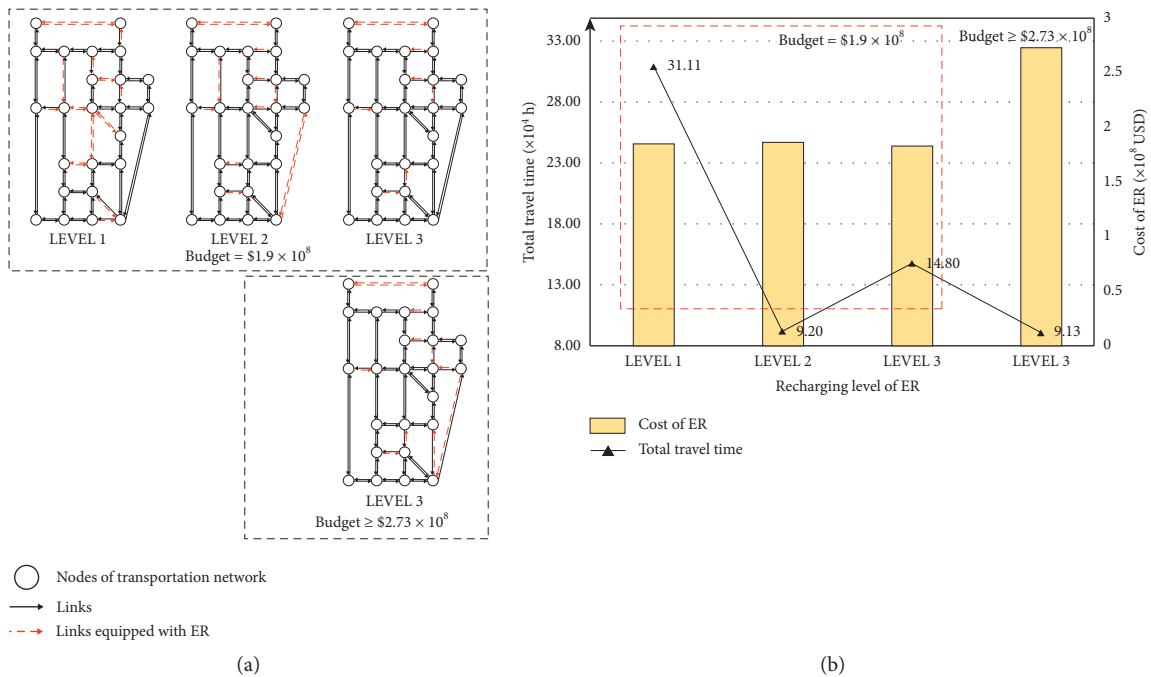


FIGURE 4: Comparison with the ER of different recharging rates. (a) Location designs. (b) Total travel time and cost of the ER.

links of the length not less than 12.5 miles are qualified to be equipped with the ER. In the case of LEVEL 3, 62 links can be chosen as the candidate location of the ER. Thus, usable paths of ER drivers and total travel time are affected. Second, the cost per unit ER increases with the rise of the recharging rate, resulting in less ER constructed giving a budget constraint. Third, the state of charge and charging behavior are affected by the recharging rate, bringing about further impact on routing behavior. When the budget exceeds

$\$2.73 \times 10^8$, total travel time of the network equipped with the ER of LEVEL 3 attains the minimum. As expected, more usable paths are generated as recharging rate increases, which may reduce the total travel time with more probable links sharing the traffic loads.

4.5. *Impacts of Comfortable Range on Location Design and System Performance.* Variations in comfortable range change the usable path sets, and thereby hinder routing choice and

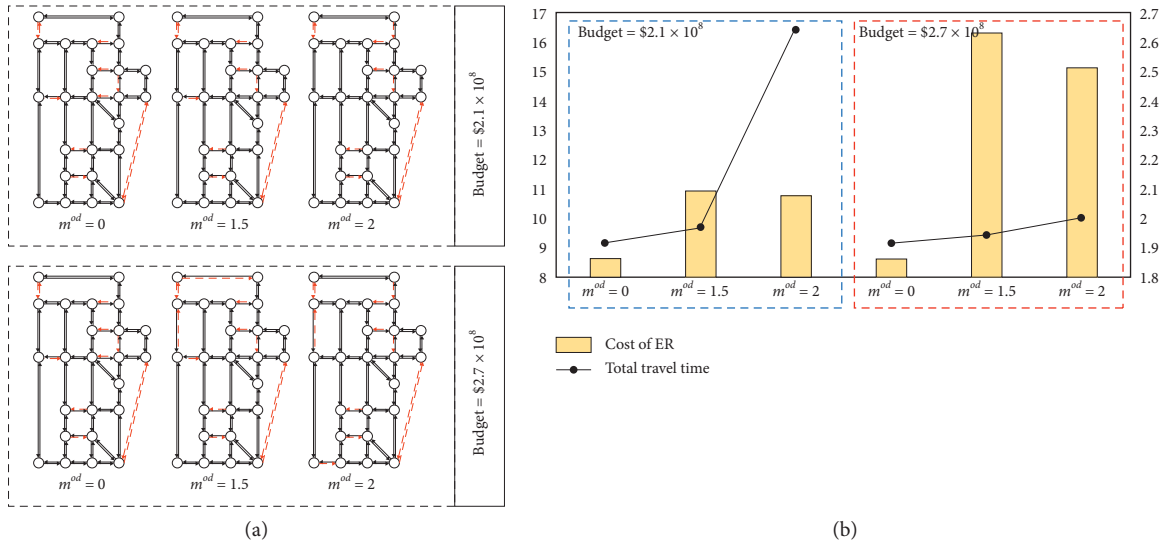


FIGURE 5: Comparison with different comfortable ranges (m^{od} : kWh). (a) Location designs (m^{od} : kWh). (b) Total travel time and cost of the ER.

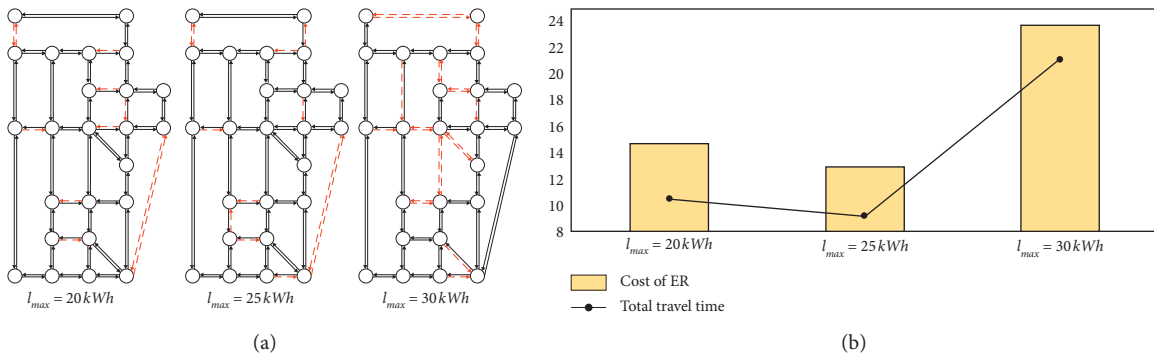


FIGURE 6: Comparison of the ER with different battery sizes. (a) Location designs. (b) Total travel time and cost of the ER.

the ER location design. In this section, the impact of comfortable range on location design and system performance is tested with DLEP of different comfortable ranges $m^{od} = 1.5$ kWh and $m^{od} = 2$ kWh under the budget limit of $\$2.1 \times 10^8$ and $\$2.7 \times 10^8$ solved, respectively, comparing with $m^{od} = 0$. Location designs of the ER are shown in Figure 5(a). Figure 5(b) compares the total travel time and cost in these six cases. Under the budget limit of $\$2.1 \times 10^8$, change of m^{od} from 0 to 2 kWh increases the total travel time by 78%. To further explore the impacts of comfortable range, we raise the budget limit to $\$2.7 \times 10^8$ and find that the variations of the total travel time with the change in comfortable range are not obvious. That is to say, under a given budget of $\$2.1 \times 10^8$, increased comfortable range leads to the increment in the total travel time. When the budget limit is set as $\$2.7 \times 10^8$, the location design of $m^{od} = 0$ is the same as that under the budget limit of $\$2.1 \times 10^8$, with the construction cost of $\$1.865 \times 10^8$. The location designs of $m^{od} = 1.5$ kWh and $m^{od} = 2$ kWh change to yield the minimum travel time, which

is close to the number when $m^{od} = 0$, with the construction cost increasing to $\$2.63 \times 10^8$ and $\$2.5 \times 10^8$, respectively.

4.6. Impacts of the Battery Size on Location Design and System Performance. Different battery sizes affect the routing choice and location design in two ways. First, the shortest length of the ER is different according to constraint (16). Second, the state of charge and charging behavior are different according to constraints (7) and (9). In this section, budget limit is set as $\$4 \times 10^8$ to explore the location design and system performance under different battery sizes $l_{max} = 20, 25$, and 30 kWh. Initial state of charge is set as $l_0 = 25\% l_{max}$. As revealed in Figure 6, location design with the battery size of $l_{max} = 25$ kWh has the least total travel time and construction cost of the ER. On the one hand, as commonly considered, a larger battery size allows more charging amount on the ER, which may generate more usable path and reduce the total travel time. On the other hand, constraint (16) sets the

minimum length of the ER which is related to the battery size. When $l_{\max} = 3$ kWh, only 26 links whose length is more than 12 miles can be the candidate of the ER, which affects the set of usable paths and the total travel time.

From the above discussion, we can find that

- (1) System total travel time of the network decreases with an increase in the budget. More ERs are built with an increasing budget, generating more usable route choice for the EV to complete the tour, which promotes average distribution of traffic flow leading to reduction in the system travel time.
- (2) Recharging rate sets the bottom boundary for the length of the candidate of the ER, which affects the EV drivers' routing choice. Besides, recharging rate is related to the construction cost, which should be balanced with the budget limit.
- (3) Increase in comfortable range changes the sets of usable path. Therefore, system travel time increases.
- (4) Battery sizes affect the shortest length of the ER as well as the initial state of charge and charging behavior, which should be balanced under different budgets.

5. Conclusion

To enhance the transportation network performance as ER is equipped, this paper proposes a LDER model to optimize the location of the ER, considering the routing and charging behavior of EV drivers by a PCNE model. EV drivers are assumed to decide their routing and recharging plan to minimize their travel time and prevent running out of charge. We develop a modified active set algorithm to obtain the optimal location of the ER. Numerical examples are conducted to demonstrate the performance of the model in comparison with the location designs in different budget limits, recharging rates, comfortable range, and battery sizes.

The energy consumption rate and the recharging rate of the proposed path-constrained network equilibrium are assumed to be flow-independent. Our future study will extend our model to investigate the effect of the traffic congestion on the energy consumption rate and the recharging rate and try to find the solution algorithm. Besides, the transportation network can be extended to accommodate both EVs and regular vehicles, with impact of the mixed traffic flow investigated.

Data Availability

The data used to support the findings of this study are available from the corresponding author upon request.

Disclosure

The authors are responsible for all views and opinions expressed in this paper.

Conflicts of Interest

The authors declare that there are no conflicts of interest regarding the publication of this paper.

Acknowledgments

This study was supported by the Joint Science Foundation of Ministry of Education of China & CMCC (Grant No. 2018202004). The first author was supported by the Program for Changjiang Scholars and Innovative Research Team in University. The third author was supported by the National Natural Science Foundation for Young Scholars of China (Grant No. 71901190).

References

- [1] C. W. Yang and Y.-L. Ho, "Assessing carbon reduction effects toward the mode shift of green transportation system," *Journal of Advanced Transportation*, vol. 50, no. 5, pp. 669–628.
- [2] P. Vorobiev and Y. Vorobiev, "About the possibilities of using the renewable energy power sources on railway transport," *Journal of Advanced Transportation*, vol. 47, no. 8, pp. 681–691, 2013.
- [3] M. D. Meyer, "Transport planning for urban areas: a retrospective look and future prospects," *Journal of Advanced Transportation*, vol. 34, no. 1, pp. 143–171, 2000.
- [4] A. Shukla and S. A. Ansari, "Energy harvesting from road pavement: a cleaner and greener alternative," *International Research Journal of Engineering and Technology (IRJET)*, vol. 5, no. 2, 2018.
- [5] A. Northmore and S. Tighe, "Innovative pavement design: are solar roads feasible?" in *Proceedings of the Conference of the Transportation Association of Canada*, Fredericton, Canada, October 2012.
- [6] A. S. Dezfooli, F. M. Nejad, H. Zakeri, and S. Kazemifard, "Solar pavement: a new emerging technology," *Solar Energy*, vol. 149, pp. 272–284, 2017.
- [7] X. Yu, S. Sandhu, S. Beiker, R. Sasso, and S. Fan, "Wireless energy transfer with the presence of metallic planes," *Applied Physics Letters*, vol. 99, no. 21, pp. 1230–1610, 2011.
- [8] P. Ning, J. M. Miller, O. C. Onar, C. P. White, and L. D. Marilino, "A compact wireless charging system development," in *Proceedings of the Twenty-Eighth Annual IEEE Applied Power Electronics Conference and Exposition (APEC)*, IEEE, Long Beach, CA, USA, March 2013.
- [9] D. U. Eberle and D. R. Von Helmolt, "Sustainable transportation based on electric vehicle concepts: a brief overview," *Energy & Environmental Science*, vol. 3, no. 6, pp. 689–699, 2010.
- [10] N. S. Pearre, W. Kempton, R. L. Guensler, and V. V. Elango, "Electric vehicles: how much range is required for a day's driving?" *Transportation Research Part C: Emerging Technologies*, vol. 19, no. 6, pp. 1171–1184, 2011.
- [11] I. E. Agency and E. V. Global, "Global ev outlook. understanding the electric vehicle landscape to 2020," 2013.
- [12] P. Bansal, "Charging of electric vehicles: technology and policy implications," *The Journal of Science Policy & Governance*, vol. 6, no. 1, p. 38, 2015.
- [13] J. U. K. Tidy, "Test wireless charging for electric car. 2015," <http://news.sky.com/story/>.
- [14] J. Ramsey, "Volvo studying test of electric roads in sweden," 2014, <http://www.autoblog.com/>.

- [15] M. Fuller, "Wireless charging in California: range, recharge, and vehicle electrification," *Transportation Research Part C: Emerging Technologies*, vol. 67, pp. 343–356, 2016.
- [16] N. Jiang, C. Xie, and T. Waller, "Path-constrained traffic assignment: model and algorithm," *Transportation Research Record Journal of the Transportation Research Board*, vol. 2283, no. 1, pp. 25–33, 2012.
- [17] N. Jiang and C. Xie, "Computing and analyzing equilibrium network flows of gasoline and electric vehicles," in *Proceedings of the Transportation Research Board 92nd Annual Meeting*, Washington, DC, USA, January 2013.
- [18] N. Jiang, C. Xie, J. C. Duthie, and S. T. Waller, "A network equilibrium analysis on destination, route and parking choices with mixed gasoline and electric vehicular flows," *EURO Journal on Transportation and Logistics*, vol. 3, no. 1, pp. 55–92, 2014.
- [19] F. He, Y. Yin, and J. Zhou, "Integrated pricing of roads and electricity enabled by wireless power transfer," *Transportation Research Part C: Emerging Technologies*, vol. 34, no. 9, pp. 1–15, 2013.
- [20] F. He, Y. Yin, J. Wang, and Y. Yang, "Sustainability SI: optimal prices of electricity at public charging stations for plug-in electric vehicles," *Networks and Spatial Economics*, vol. 16, no. 1, pp. 131–154, 2016.
- [21] F. He, D. Wu, Y. Yin, and Y. Guan, "Optimal deployment of public charging stations for plug-in hybrid electric vehicles," *Transportation Research Part B: Methodological*, vol. 47, no. 1, pp. 87–101, 2013.
- [22] F. He, Y. Yin, and J. Zhou, "Deploying public charging stations for electric vehicles on urban road networks," *Transportation Research Part C: Emerging Technologies*, vol. 60, pp. 227–240, 2015.
- [23] F. He, Y. Yin, and S. Lawphongpanich, "Network equilibrium models with battery electric vehicles," *Transportation Research Part B: Methodological*, vol. 67, no. 3, pp. 306–319, 2014.
- [24] M. Xu, Q. Meng, and K. Liu, "Network user equilibrium problems for the mixed battery electric vehicles and gasoline vehicles subject to battery swapping stations and road grade constraints," *Transportation Research Part B: Methodological*, vol. 99, pp. 138–166, 2017.
- [25] R. Riemann, D. Z. W. Wang, and F. Busch, "Optimal location of wireless charging facilities for electric vehicles: flow-capturing location model with stochastic user equilibrium," *Transportation Research Part C: Emerging Technologies*, vol. 58, pp. 1–12, 2015.
- [26] Z. Chen, F. He, and Y. Yin, "Optimal deployment of charging lanes for electric vehicles in transportation networks," *Transportation Research Part B: Methodological*, vol. 91, pp. 344–365, 2016.
- [27] Z. Chen, W. Liu, and Y. Yin, "Deployment of stationary and dynamic charging infrastructure for electric vehicles along traffic corridors," *Transportation Research Part C: Emerging Technologies*, vol. 77, pp. 185–206, 2017.
- [28] Z. Liu and Z. Song, "Robust planning of dynamic wireless charging infrastructure for battery electric buses," *Transportation Research Part C: Emerging Technologies*, vol. 83, pp. 77–103, 2017.
- [29] Z. Liu, Z. Song, and Y. He, "Optimal deployment of dynamic wireless charging facilities for an electric bus system," *Transportation Research Record: Journal of the Transportation Research Board*, vol. 2647, no. 1, pp. 100–108, 2017.
- [30] A. S. Ahmed, A. M. Mohamed, and Z. H. U. Lei, "System design and optimization of in-route wireless charging infrastructure for shared automated electric vehicles," *IEEE Access*, vol. 7, pp. 79968–79979, 2019.
- [31] Z. Bi, G. A. Keoleian, Z. Lin et al., "Life cycle assessment and tempo-spatial optimization of deploying dynamic wireless charging technology for electric cars," *Transportation Research Part C: Emerging Technologies*, vol. 100, pp. 53–67, 2019.
- [32] T. Zhao, Z. Wu, and Y. Zhang, "Bi-objective optimization of electric bus dynamic wireless charging facilities location and onboard battery size considering both facility cost and energy consumption," in *Proceedings of the Transportation Research Board 98th Annual Meeting*, Washington, DC, USA, January 2019.
- [33] L. J. Leblanc, "An algorithm for the discrete network design problem," *Transportation Science*, vol. 9, no. 3, pp. 183–199, 1975.
- [34] T. L. Friesz, H.-J. Cho, N. J. Mehta, R. L. Tobin, and G. A. Nandalingam, "A simulated annealing approach to the network design problem with variational inequality constraints," *Informatics*, vol. 26, no. 1, pp. 18–26, 1992.
- [35] S. Wang, Q. Meng, and H. Yang, "Global optimization methods for the discrete network design problem," *Transportation Research Part B Methodological*, vol. 50, pp. 42–60.
- [36] L. Zhang, S. Lawphongpanich, and Y. Yin, *An Active-Set Algorithm for Discrete Network Design Problems*, Springer Science+Business Media, Berlin, Germany, 2009.